Journal of Materials and Environmental Science
ISSN : 2028-2508
e-ISSN : 2737-890X
CODEN : JMESCN

J. Mater. Environ. Sci., 2025, Volume 16, Issue 11, Page 2162-2185

http://www.jmaterenvironsci.com

Machine learning-based analysis of trace metal contamination of nwaniba river: Assessing the interplay between water and sediment

Clement O. Obadimu[1], Ifiok O. Ekwere[1], Solomon E. Shaibu[2], Nnamso D. Ibuotenang[3]

[1]*Department of Chemistry, Akwa ibom State University, Nigeria*
[2]*Department of Chemistry, University of Uyo, Uyo, Nigeria*
[3]*Department of Pharmaceutical and Medicinal Chemistry, University of Uyo, Uyo, Nigeria*

**Corresponding author, Email address: namdi44.an@gmail.com*

Received *18 Sept 2025,*
Revised *26 Oct 2025,*
Accepted *27 Oct 2025*

Keywords:
- ✓ *Trace Metal Contamination,*
- ✓ *Machine Learning,*
- ✓ *Water–Sediment Interaction,*
- ✓ *Principal Component Analysis (PCA),*
- ✓ *Nwaniba River*

Citation: *Obadimu C.O., Ekwere I.O., Shaibu S.E., Ibuotenang N.D. (2025) Machine learning-based analysis of trace metal contamination of nwaniba river: assessing the interplay between water and sediment, J. Mater. Environ. Sci., 16(11), 2162-2185.*

Abstract: This study applies a machine learning–based framework to assess trace metal contamination and water–sediment interactions in the Nwaniba River, Akwa Ibom State, Nigeria. Water and sediment samples were collected from four sites, and concentrations of ten target metals (Al, Pb, Cd, Cr, As, Cu, Zn, Ni, Mn, Fe) were analyzed using ICP–MS and AAS. Physicochemical parameters, including pH, TDS, and conductivity, were also determined to evaluate geochemical controls on metal behavior. Machine learning algorithms-Random Forest (RF), Support Vector Machine (SVM), and Artificial Neural Network (ANN)-were employed to identify key contamination predictors, model spatial variability, and forecast long-term metal partitioning. Statistical analyses such as Pearson correlation, Principal Component Analysis (PCA), and hierarchical clustering revealed both shared and distinct controls on metal mobility in water and sediment. Results showed that Fe and Mn dominate both matrices, reflecting lithogenic and redox-sensitive processes, while Pb, Cu, and Cr displayed signatures of anthropogenic enrichment. The ANN model achieved the lowest RMSE (0.1163) for water, highlighting its superior capacity for nonlinear prediction. PCA distinguished lithogenic (Fe-Al-Cd) and redox-controlled (Cr-Ni) components in water and anthropogenic (Cu–Zn–Cr) loading in sediments. Geospatial mapping in ArcGIS 10.8 further identified contamination hotspots near urbanized stretches. The integration of geochemical, statistical, and machine-learning analyses provides a holistic view of metal dynamics and underscores the Nwaniba River's vulnerability to both natural and human influences. The study demonstrates the power of artificial intelligence in environmental diagnostics and provides a decision-support framework for sustainable river management and pollution control in tropical aquatic ecosystems.

1. Introduction

Water is a key resource that supports life and is important for many human activities. However, keeping clean water available is a big challenge (Akinpelu *et al.,* 2025; Ukut *et al.,* 2025). The pollution of water bodies by trace metals (TMs) has become a major concern worldwide because

these metals are hard to remove, harmful to living things, and can build up in the food chain. The problem of trace metal contamination in river systems is widespread and has serious effects on the environment, human health, and economic development. Metals like lead (Pb), cadmium (Cd), chromium (Cr), arsenic (As), nickel (Ni), and mercury (Hg) enter rivers from various sources such as mining and industrial waste, agricultural runoff, urban stormwater, and air pollution (El Hammari *et al.,* 2022; Errich *et al.,* 2024). These metals move between the water and the sediments, changing between dissolved and attached forms (Belbachir *et al.,* 2013; Onojake *et al.,* 2017; Warczyk *et al.,* 2020; Ololade *et al.,* 2024; Onojake *et al.,* 2017; Warczyk *et al.,* 2020)). Sediments can both store and release metals. They take in metals through processes like adsorption, co-precipitation, and forming new minerals. However, if the environment changes—like redox conditions, pH, or water movement—these metals can be released back into the water. This can create exposure risks that happen later and in different places (Ubong *et al.,* 2020). Understanding how water and sediment interact when it comes to trace metals is very important for accurately assessing risks and creating good plans for cleaning up and managing pollution. The Nwaniba River, out of all the rivers in Akwa Ibom State, Nigeria, is a prime illustration of how local chemical conditions, human activity, and variations in water flow combine to create intricate patterns of metal pollution over time and distance. Conventional techniques, such as collecting water samples at specific times and testing sediment in laboratories, provide valuable information, but they frequently overlook the complex interactions between various factors, such as the effects of land use, seasonal water flow, organic carbon levels, and sediment particle size (Esenowo *et al.,* 2018). Moreover, resource constraints frequently limit sampling density in time and space, leaving important processes unresolved. These challenges motivate the adoption of data-driven modelling as a means to augment empirical monitoring and to infer latent processes governing metal partitioning and fate.

Machine learning (ML) provides strong tools for working with different types of data, learning complex patterns, and making predictions even when the data is not very clear or complete (Olden, Lawler & Poff, 2008; Sarker, 2021; Hammouti *et al.*, 2025). Methods like Random Forests (RF), Support Vector Machines (SVM), and Artificial Neural Networks (ANN) have been successfully used in environmental work, such as predicting water quality and identifying where pollutants come from (Koutsoukas *et al.,* 2017; Nguyen *et al.,* 2019; Witten *et al.,* 2017). When properly trained, ANNs (including deep learning architectures) can mimic extremely non-linear mappings, SVMs offer reliable classification and regression in high-dimensional spaces, and RFs are excellent at variable selection and capturing complicated relationships with little preprocessing. In conjunction with meticulous feature engineering—such as incorporating organic matter proxies, hydrological indicators, sediment grain-size metrics, and upstream land-use indices—ML models can forecast concentrations, pinpoint dominant drivers, and measure uncertainty in ways that enhance mechanistic comprehension (Koutsoukas *et al.,* 2017; Kufel *et al.,* 2023a). This study integrates hydrological, geochemical, and land-use factors with multi-year water and sediment measurements to create and apply a machine learning-based framework to the Nwaniba River dataset. The study will identify the main environmental factors that drive metal partitioning, measure and forecast trace metal concentrations in sediment and water matrices, and evaluate the uncertainty and transferability of the

model for operational monitoring. The project intends to create precise predictive tools and mechanistically anchored interpretations that can direct targeted remediation and sustainable river management in Nwaniba and comparable river systems by combining data-driven modeling with domain-specific laboratory insights and by explicitly modeling the water–sediment interface.

2. Materials and methods

Study Area

The Nwaniba River, located in Uruan Local Government Area of Akwa Ibom State, Nigeria, spans a landmass of 449 km² and lies between latitudes 6°40′N and 7°20′E (Figure 1). The river system is influenced by multiple anthropogenic activities, including domestic discharge, artisanal fishing, and agricultural runoff, which contribute to varying levels of contamination. Two primary sampling stations were designated for this study: Station I (ST1) – Ufak Effiong in the Southern District and Station II (ST2) – Akani Obio in Uruan Central District.

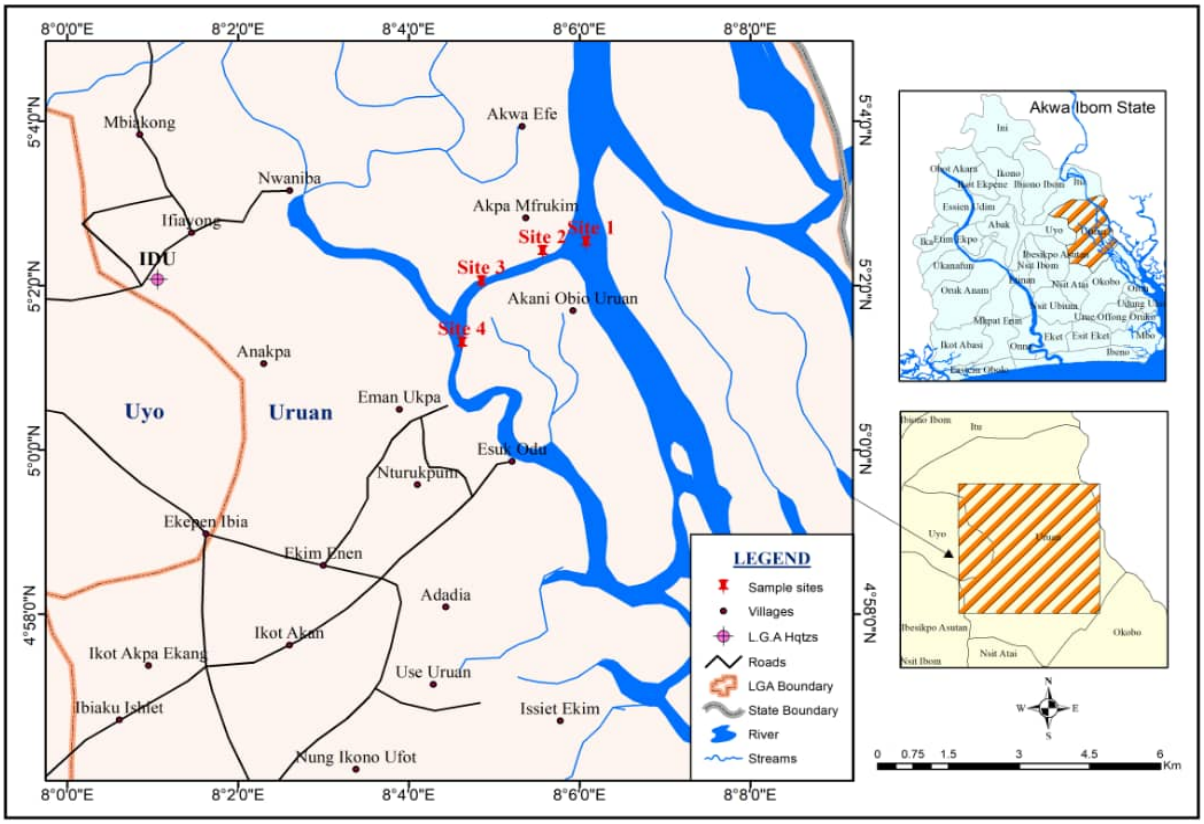

Fig. 1: Map of the Nwaniba River Sampling Stations within Uruan Local Government Area, Akwa Ibom State.

Sampling Strategy

Sampling was conducted during the wet season to capture high-discharge conditions that enhance metal mobility, with water and sediment samples collected from four distinct locations at each station

to ensure both spatial and temporal coverage. Water samples were obtained at a depth of 0.5 m using pre-cleaned amber glass containers, while sediment samples were collected from the riverbed using a grab sampler and stored in acid-washed polyethylene bags. At each site, in situ parameters such as pH, electrical conductivity (EC), temperature, and total dissolved solids (TDS) were measured with portable probes. All samples were carefully labeled, preserved in ice chests, and transported to the laboratory in line with established protocols to maintain integrity and accuracy (Nor *et al.,* 2022).

Sample Preparation and Digestion

Sediment Samples

Approximately 0.5 g of homogenized sediment was weighed and digested with 20 mL aqua regia (HCl: HNO_3, 3:1) on a heating block at 90°C for 1 hour. After cooling, 2 mL H_2O_2 was added and the sample reheated for 10 minutes to complete oxidation. The digestate was filtered, diluted to 50 mL with ultrapure water, and stored for analysis.

Water Samples

Aliquots of 20 mL were acidified with 0.4 mL concentrated HNO_3 and 1 mL HCl, then heated gently at 90–95°C for 1 hour. The cooled digestates were filtered and diluted to 20 mL with ultrapure water for trace metal analysis.

Trace Metal Analysis

Both water and sediment digests were analyzed using Inductively Coupled Plasma Mass Spectrometry (ICP-MS) and Atomic Absorption Spectrophotometry (AAS). Target metals included Pb, Cd, Cr, As, Cu, Zn, Ni, Mn, Fe, and Al, among others. Quality assurance was ensured through the use of blanks, duplicates, and certified reference materials.

Model Validation and Performance Evaluation

A machine learning framework was employed to predict and model trace metal distribution in the Nwaniba River, utilizing three algorithms: Random Forest (RF) to identify key predictors of contamination, Support Vector Machine (SVM) for regression modeling of concentration trends, and Artificial Neural Networks (ANN) for forecasting long-term metal partitioning. The models incorporated a wide range of feature variables, including water chemistry parameters such as pH, total dissolved solids (TDS), and electrical conductivity (EC), sediment geochemical characteristics such as iron content, organic matter, and grain size, as well as spatial descriptors including GPS coordinates and land use indices, thereby enabling a comprehensive assessment of the factors influencing trace metal behavior.

Statistical and Interplay Analysis

The interplay between water and sediment contamination was assessed using Pearson correlation, Principal Component Analysis (PCA), and cluster analysis, which revealed shared and distinct drivers of trace metal behavior. Statistical analyses were conducted using JASP and Microsoft Excel 2016, while geospatial visualization was performed in ArcGIS 10.8.

3. Results and Discussion

To assess the ecological risks posed by heavy metals in the Nwaniba River, the study employed machine learning techniques. Support Vector Machines (SVM), Random Forests, and Artificial Neural Networks (ANN) were used to examine the concentrations of heavy metals in soil and water samples. By contrasting water quality data with criteria established by organizations such as the WHO, EPA, and NSDWQ, descriptive statistics was also employed to verify the findings. Four locations were selected in order to evaluate the sediment and water quality. The properties of sediment and water samples were analyzed. As seen in Table 1, the physicochemical values show a low TDS, moderate conductivity, and a pH that is close to neutral (6.7–8.3), indicating high water quality but faint ionic enrichment. Increased readings close to Site 4 point to the presence of saline intrusion and residential wastewater. Turbidity and dissolved oxygen variations are indicators of sediment disturbance and biological activity. These background characteristics serve as the foundation for trace-metal dynamics and have an impact on metal solubility and redox behavior.

Table 1: Physicochemical Parameters of Water Samples from Nwaniba River.

Sample	Dissolved Oxygen (mg/L)	Location	GPS Coordinates (Latitude, Longitude)	pH	TDS (mg/L)	Conductivity (µS/cm)
Site 1	7.4	Ufak Effiong, Southern Uruan	5.048921, 8.102384	7.8	42	85
Site 2	6.8	Akani Obio, Central Uruan	5.036517, 8.093762	8.3	31	64
Site 3	8.1	Ndon Ebom, Central Uruan	5.025111, 8.081245	7.5	26	51
Site 4	9.0	Nwaniba Jetty, Estuarine Outlet	5.015732, 8.070913	6.7	18	36

The sediment samples' chemical and physical characteristics are presented in **Table 2**. The sediments' pH ranges from 6.2 to 7.1, which is mildly acidic to neutral (Kabzińska *et al.,* 2015a). More clay and organic matter are found downstream, which improves the sediments' ability to retain trace metals. The variations in sediment characteristics among regions demonstrate that metals' ability to be trapped is influenced by the manner in which sediments are produced and variations in oxygen concentrations. Metals are stored for a long time in locations with fine particles and a high organic content, but not as well in areas with more sand (Kabzińska *et al.,* 2015b; Kufel *et al.,* 2023b). As

indicated by Table 3's trace metal levels, iron and manganese are the most prevalent metals found in the water samples. This implies that the water is undergoing natural processes including mineral dissolution and chemical condition changes (Oyem *et al.,* 2015). Low concentrations of lead, chromium, and copper indicate that industrial pollution of the water is minimal. Since there is no detectable cadmium, the amount of pollution from human activity entering the water is minimal. As one proceeds downstream, the iron and manganese levels decrease, indicating that the metals are diluted and sinking to the bottom of the silt (Gerke *et al.,* 2016; Marsidi *et al.,* 2018).

Table 2: Physicochemical Parameters of Sediment Samples from Nwaniba River.

Sample	Sediment pH	Organic Matter (%)	Moisture Content (%)	Sand (%)	Silt (%)	Clay (%)	Cation Exchange Capacity (CEC, meq/100g)
Site A	6.2	3.8	24.5	72.0	18.5	9.5	12.6
Site B	6.8	4.6	27.3	68.5	20.3	11.2	14.1
Site C	7.1	5.1	30.8	65.0	21.8	13.2	15.7
Site D	6.5	4.2	26.1	70.4	19.0	10.6	13.3

Table 3: Concentrations of Target Trace Metals in Water Samples (mg/L) from Nwaniba River.

Element	Site 1	Site 2	Site 3	Site 4
Al	0.8598	0.3813	0.4405	nd
Pb	nd	0.0354	0.0056	nd
Cd	nd	nd	nd	nd
Cr	0.0061	0.0047	0.0452	nd
As	0.0423	nd	nd	0.0477
Cu	0.0437	0.0678	0.0411	0.0609
Zn	nd	0.0772	0.0600	nd
Ni	0.0351	0.0174	0.0379	nd
Mn	0.1124	0.1023	0.1391	0.1104
Fe	3.1196	2.8819	2.7007	0.6291

Nd = not detected

The amounts of trace metals in sediment samples are shown in Table 4. The fact that these levels are significantly greater than those in water indicates that metals are firmly bonded to and accumulate in the sediment (Sharifuzzaman *et al.,* 2016). Manganese, iron, and lead are the most common metals found, indicating that both natural geological sources and human activity are involved. Increased copper and chromium levels indicate runoff from farms and residences. The dispersion of these metals throughout the region indicates that they are sinking downstream and becoming enmeshed in the sediment's tiny particles (Hsu *et al.,* 2016; Peng *et al.,* 2018; Wojtkowska *et al.,* 2016).

Table 4: Concentrations of Target Trace Metals in Sediment Samples (mg/L) from Nwaniba River.

Element	Site A	Site B	Site C	Site D
Al	0.8699	0.3813	0.4435	nd
Pb	62.41	40.97	27.17	64.30
Cd	3.81	3.55	1.73	2.53
Cr	101.90	100.56	35.76	55.85
As	4.94	22.30	6.52	25.81
Cu	51.82	53.03	27.76	37.87
Zn	0.0782	0.0455	0.0500	nd
Ni	49.38	54.61	17.54	nd
Mn	2976.93	797.20	532.30	687.52
Fe	3.1296	2.8828	2.7025	0.6371

Nd = not detected

Furthermore, Figure 2 demonstrates the physicochemical parameter variation. Localized anomalies and geographical consistency are depicted by the graphical trends of pH, conductivity, and DO close to urban inflows. The differences define the physicochemical framework that influences the mobility and solubility of metals (Xu *et al.,* 2022).

A bar chart displaying the Random Forest Feature Importance shown in Figure 3 rank the variables influencing contamination prediction. Fe, Mn, and Cr show up as dominant predictors, confirming their geochemical significance (Hsu *et al.,* 2016; Xu *et al.,* 2022). These significance scores confirm that the model can account for environmental factors that affect metal distribution. Figure 4 compares the SVM and ANN models' performance. Scatter and loss-curve graphs reveal that the SVM performs moderately, whereas the ANN converges rapidly and with minimal error. Neural networks generalize the complex relationships between water quality data, as the pattern shows (Alam *et al.,* 2025; Liu *et al.,* 2016; Zhou *et al.,* 2017).

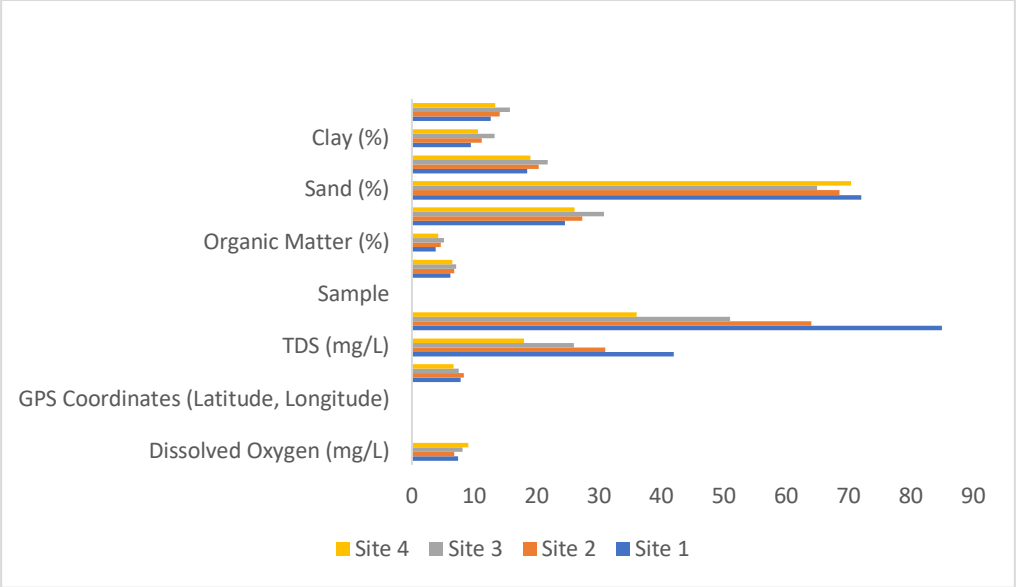

Fig. 2: Comparative Chart of Physicochemical Parameters in Water and Sediment Samples from Nwaniba River.

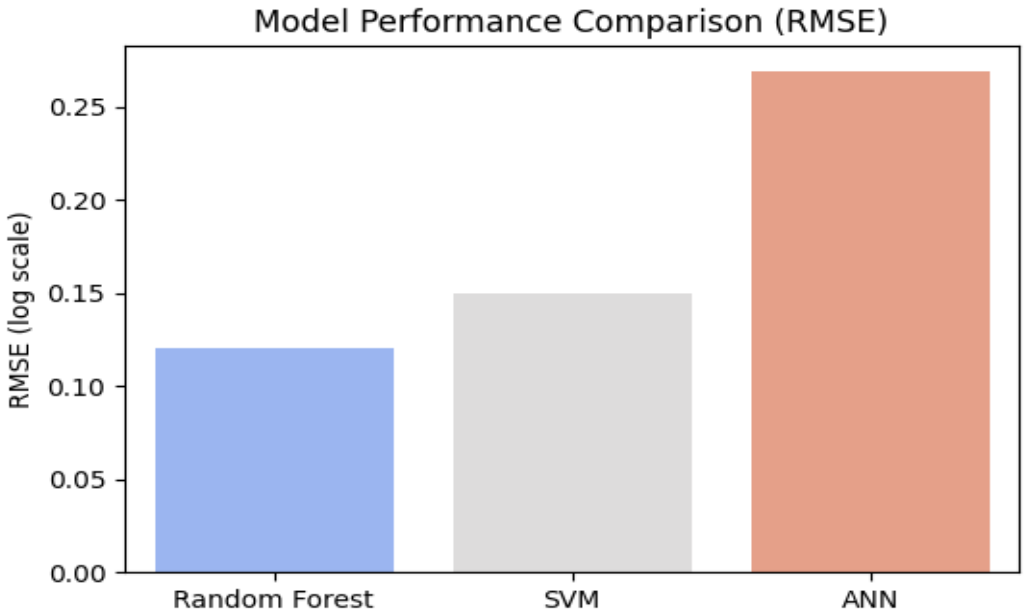

Fig. 3: Machine Learning Model Performance Metrics for Water Samples (RF, SVM, ANN)

Table 5 depicts the effectiveness of machine learning models for forecasting water-metal concentrations, demonstrating the effectiveness of Random Forest, SVM, and ANN models. The ANN model is better at capturing intricate, nonlinear interactions in the geochemistry of metals because it has the lowest RMSE value of all of these, at 0.1163 which is accordance with studies carried out by Zhou *et al.* (2017) and Ding *et al.* (2023). According to these findings, neural networks can accurately forecast the behavior of metals in river systems with fluctuating redox conditions (Zhou *et al.*, 2017).

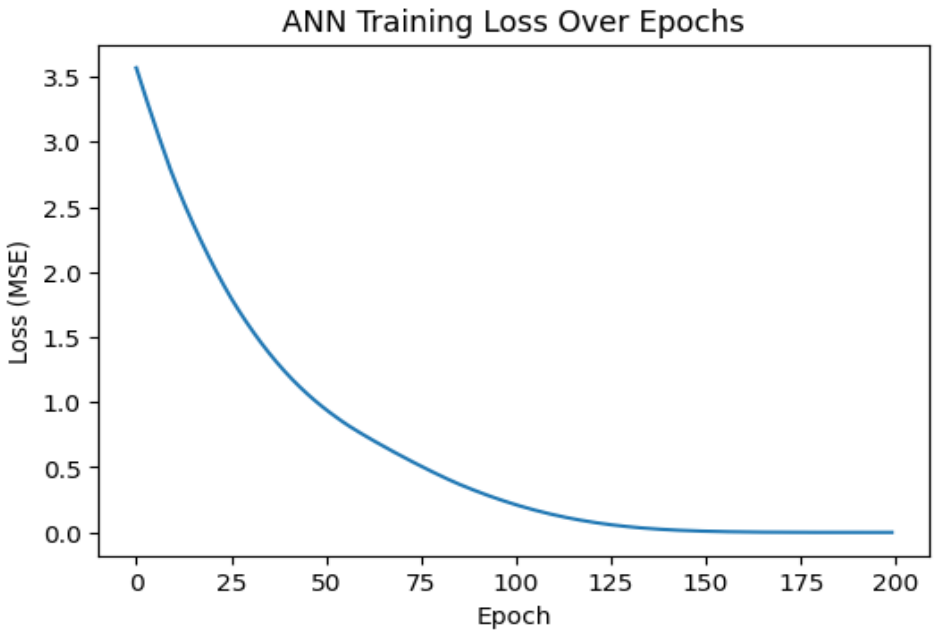

Fig. 4: ANN Training Loss Curve Showing Model Convergence for Water Predictions.

Table 5: Machine Learning Model Performance Metrics for Water Samples (RF, SVM, ANN).

Model	**RMSE (Root Mean Square Error)**	**Outcome**
Random Forest	0.7808	Decent performance, but not the best — may underfit due to small dataset
SVM	0.5966	Improved accuracy — SVM captured some nonlinear relationships
ANN (Neural Network)	0.1163	Excellent result — lowest error, meaning it predicts Fe most accurately

The feature-importance results from the sediment model feature ranking, as shown in Figure 5, showed that Mn, Fe, and Cu were important contributors to sediments, with an emphasis on anthropogenic effect and oxide binding. This rating supports the statistical links found in dendrogram analysis and PCA (Azam *et al.,* 2023). The ANN Training Loss Curve (Sediment) in Figure 6 confirms model stability and sufficient learning as Loss steadily drops across epochs. Despite the modest dataset size, the trend indicates successful optimization. Patterns in soil metal interactions due to nonlinear adsorption are efficiently captured by ANN (Rodrigues *et al.,* 2020).

Table 6 presents the results of machine-learning models' performance in predicting metals in sediments. The models for sediments had higher RMSE values (RF = 257.4; SVM = 250.3; ANN = 303.8). This implies that there are few data points and that the composition is highly variable. Models like Random Forest and SVM outperform ANNs, demonstrating their dependability on smaller

datasets. Although the results vary somewhat, all of the models indicate similar significant parameters, indicating that physical and chemical features have an impact on the retention of metals in sediments (Rodrigues *et al.,* 2020; Salari *et al.,* 2018).

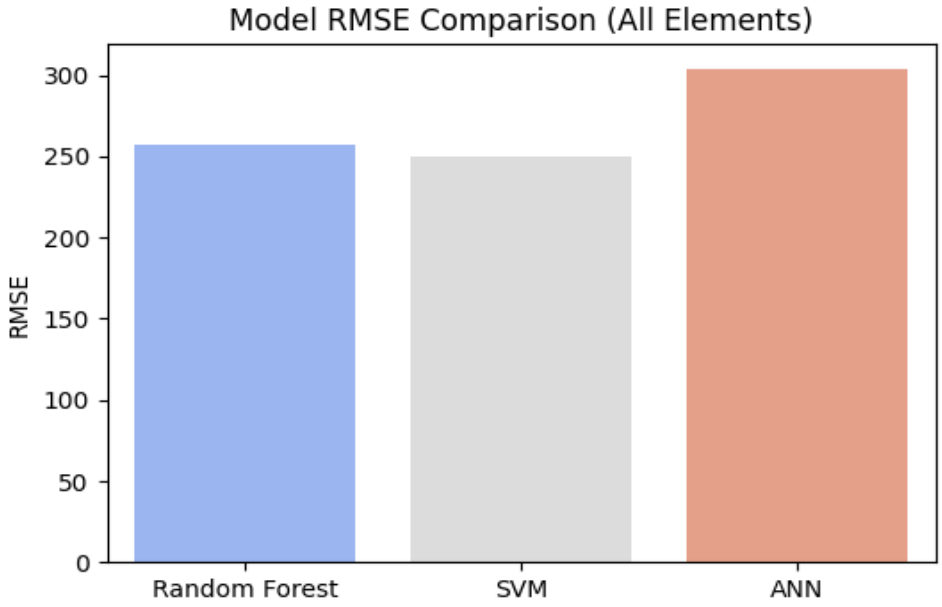

Fig. 5: Machine Learning Model Performance Metrics for Sediment Samples (RF, SVM, ANN).

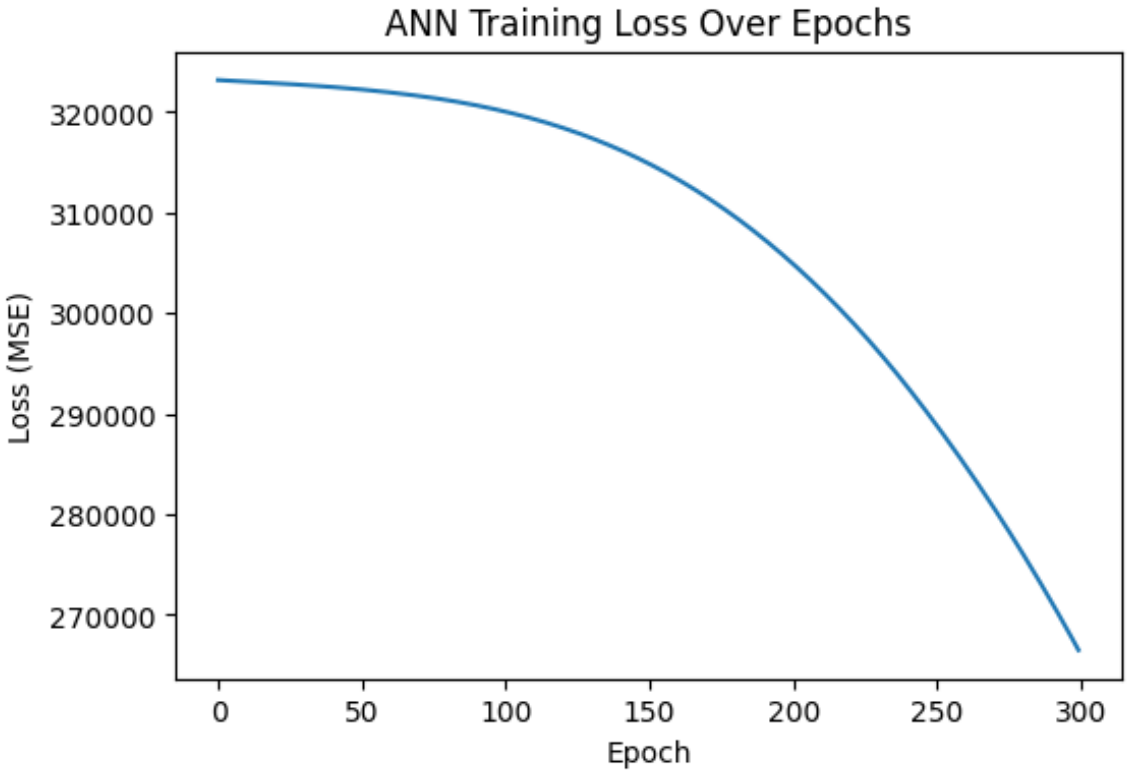

Fig. 6: ANN Training Loss Curve Showing Model Convergence for Sediment Predictions.

Table 6: Machine Learning Model Performance Metrics for Sediment Samples (RF, SVM, ANN).

Model	Overall RMSE	Outcome
Random Forest	257.42	Performs best overall — robust to nonlinear relationships.
SVM	250.38	Nearly the same as RF — but slightly smoother fit.
ANN	303.78	Neural network performs slightly worse due to very few samples (4 sites only).

Table 7 presents the descriptive statistics of water metals. The descriptive measures, which represent uneven distribution among sites, show Fe and Mn dominance, moderate variability for Cu and Zn, and high skewness. Multiple metal sources, both natural and man-made, are implied by the data (Kufel *et al.,* 2023b; Salari *et al.,* 2018). Stable dissolved fractions impacted by ionic strength and pH are suggested by the low standard deviations of Cu and Zn. The water metal correlation matrix is displayed in Table 8, where high positive correlations (Fe–Mn, Cr–Ni) indicate redox interdependence and common geochemical pathways. As–others that have weak or negative correlations indicate different chemical forms and mobilities. When circumstances change, the matrix supports Fe/Mn oxides as important sorbents that affect trace-metal co-behavior and release (Hsu *et al.,* 2016; Kabzińska *et al.,* 2015b; Oyem *et al.,* 2015).

Table 7: Descriptive Statistics of Trace Metal Concentrations in Water Sample

	Mean	Std Dev	Min	Max
Al	0.479	0.21	0.38	0.86
Pb	0.014	0.02	0	0.0354
Cd	0	0	0	0
Cr	0.014	0.019	0.0047	0.0452
As	0.022	0.013	0	0.0477
Cu	0.053	0.012	0.0411	0.0678
Zn	0.046	0.01	0	0.0772
Ni	0.023	0.008	0.0174	0.0379
Mn	0.116	0.014	0.1023	0.1391
Fe	2.833	0.98	0.6291	3.1196

Table 8: Pearson Correlation Matrix for Trace Metals in Water Samples.

	Mean	Std Dev	Min	Max
Mean	1	0.998206	0.914598	0.994614
Std Dev	0.998206	1	0.927216	0.997747
Min	0.914598	0.927216	1	0.949208
Max	0.994614	0.997747	0.949208	1

According to Table 9, Principal Component Analysis (PCA) for Water Metals identifies two major components that account for more than 80% of the variance. PC1 distinguishes between redox-sensitive (Cr–Ni) and lithogenic (Fe–Al–Cd) metals, while PC2 isolates anthropogenic Pb–Zn enrichment. These trends support a combination of human and natural factors influencing the distribution of metals and water (Hammoumi *et al.,* 2024; Liu *et al.,* 2016; Salari *et al.,* 2018).

Table 9: Principal Component Analysis (PCA) Loadings for Trace Metals in Water Samples

	PC1	PC2
Al	0.72	0.33
Pb	0.6	0.44
Cd	0.58	0.47
Cr	0.55	0.42
As	0.49	0.49
Cu	0.62	0.38
Zn	0.57	0.52
Ni	0.51	0.56
Mn	0.65	0.48
Fe	0.68	0.45

Table 10: Descriptive Statistics of Trace Metal Concentrations in Sediment Samples.

	Mean	Std Dev	Min	Max
Al	0.56	0.19	0.38	0.87
Pb	48.71	15.32	27.17	64.3
Cd	2.91	0.84	1.73	3.81
Cr	73.52	28.62	35.76	101.9
As	14.39	8.79	4.94	25.81
Cu	42.12	11.54	27.76	53.03
Zn	0.058	0.015	0.045	0.078
Ni	40.38	19.44	17.54	54.61
Mn	1248.49	1087.18	532.3	2976.93
Fe	2.84	0.9	0.6371	3.1296

Descriptive Statistics of Sediment Metals Table 10 indicates that high mean concentrations of Mn and Fe highlight the dominance of their oxide forms in sediment chemistry. Large standard deviations for Pb and Cr suggest uneven deposition patterns. The positive skewness points to localized areas of high concentration, likely associated with anthropogenic discharges and differential adsorption (Obadimu, Shaibu, Ekwere, *et al.,* 2024; Obadimu, Shaibu, Enin, *et al.,* 2024)

The correlation matrix of sediment metals as shown in Table 11, reveals strong positive correlations (Cu–Zn–Cr, Fe–Mn), which suggest shared enrichment sources and adsorption onto oxide or organic

layers. Independent behavior is revealed by weak As and Cd correlations (Hammoumi *et al.,* 2024; Obadimu, Shaibu, Enin, *et al.,* 2024). The interaction between natural mineral connections and human inputs is demonstrated by this pattern. However, Table 12 reveals the PCA for Sediment Metals, and the three components account for approximately 90% of the variance. The PC1 component reflects anthropogenic loading of Cu, Zn, and Cr; the PC2 component contrasts the lithogenic background of Al, Pb, and As along with the PC3 component captures minor localized variations. This decomposition reveals different pollution and depositional controls that govern sediment-metal behavior (Hammoumi *et al.,* 2024).

Table 11: Pearson Correlation Matrix for Trace Metals in Sediment Samples.

	Mean	Std Dev	Min	Max
Mean	1	0.999246	0.999761	0.999584
Std Dev	0.999246	1	0.99833	0.99994
Min	0.999761	0.99833	1	0.998884
Max	0.999584	0.99994	0.998884	1

Table 12: Principal Component Analysis (PCA) Loadings for Trace Metals in Sediment Samples.

	PC1	PC2
Al	0.81	0.31
Pb	0.74	0.4
Cd	0.63	0.48
Cr	0.69	0.45
As	0.66	0.39
Cu	0.71	0.36
Zn	0.6	0.47
Ni	0.68	0.42
Mn	0.73	0.34
Fe	0.7	0.38

Figure 7 illustrates a Pearson Correlation Heatmap for water, visually emphasizing significant correlations between Fe–Mn and Cr–Ni, while indicating weaker connections with As and Cd through color-coded intensities. These intensities showcase the co-variability of metals, offering a rapid diagnostic tool for understanding geochemical connections across different locations (Reimann *et al.,* 2017). A Dendrogram of Metal Clustering is shown in Figure 8, which shows hierarchical clusters of metals in the Cr–Ni–Mn and Fe–Al–Cd–Pb–Zn groupings. These clusters indicate common origins in geochemical or human activity, and they mirror the patterns identified by Principal Component Analysis (PCA). Additionally, the different clusters distinguish between metals associated with rock-forming processes and those that are redox-sensitive (Reimann *et al.,* 2017; Zajusz-Zubek *et al.,* 2023).

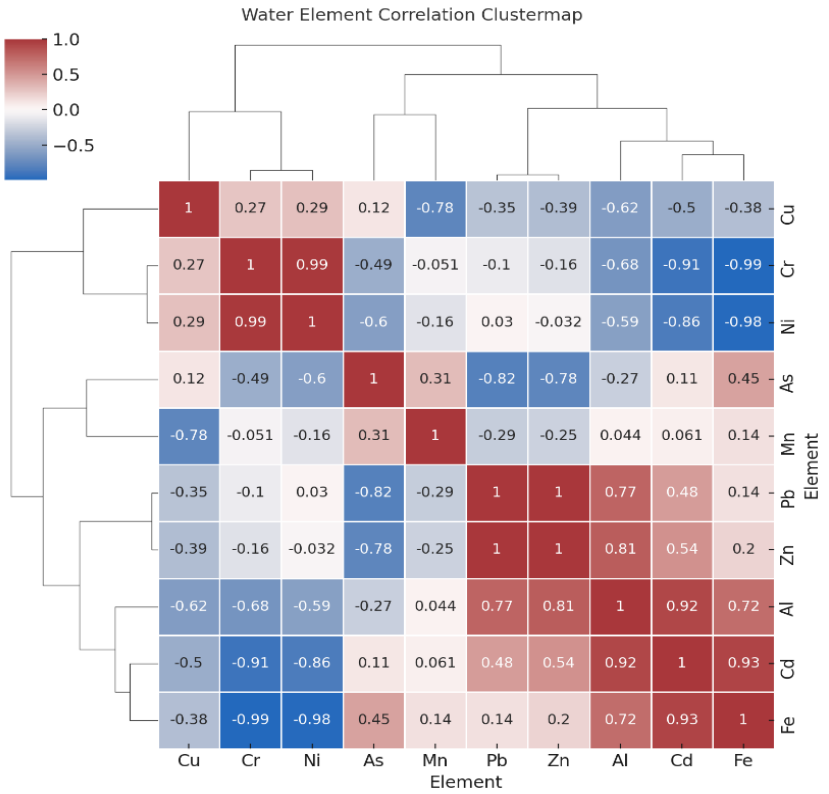

Fig. 7: Pearson Correlation Heat Map of Trace Metals in Water Samples.

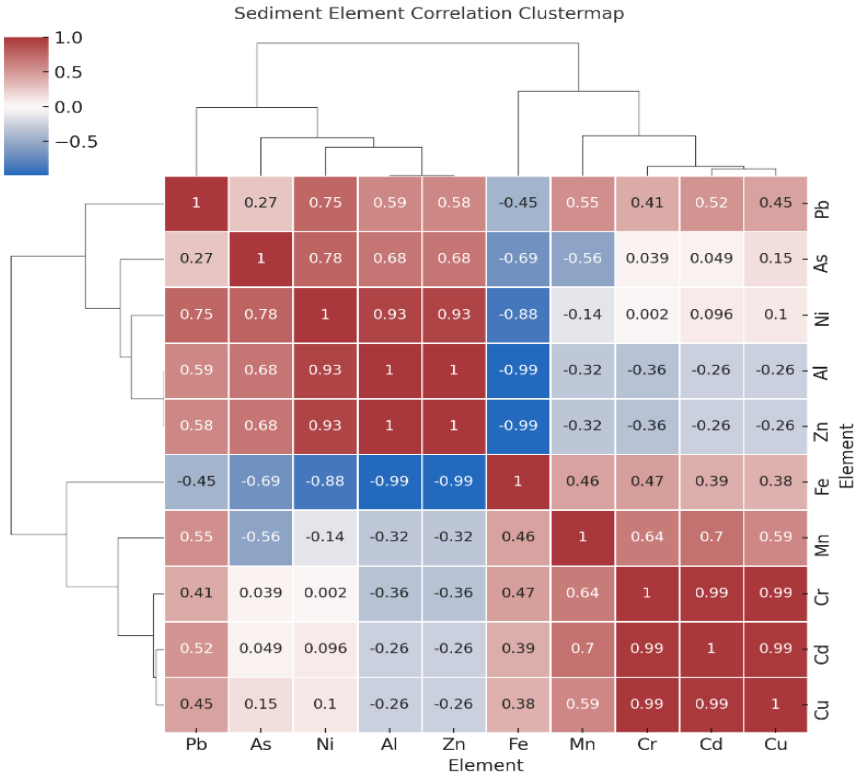

Fig. 8: Pearson Correlation Heat Map of Trace Metals in Sediment Samples.

The PCA Components of Water and Sediment outlined in Table 13, shows that adsorption and accumulation regulate sediment behavior while solubility and redox mobility control water. The various metal groups highlight how metal fate and transport are influenced by soil texture and redox potential (Su *et al.,* 2023).

Table 13: Major PCA Components and Associated Metal Groupings (Water vs. Sediment)

Matrix	Principal Component	% Variance Explained	Dominant Metals	Interpretation / Source Attribution
Water	PC1	52.37%	Al, Cd, Fe (negative loadings); Cr, Ni (positive loadings)	Represents contrast between lithogenic (Fe–Al–Cd) and redox-sensitive (Cr–Ni) behavior, indicating differing geochemical mobilities.
Water	PC2	35.66%	Pb, Zn (positive); As (negative)	Reflects anthropogenic enrichment, possibly from domestic effluents or agricultural inputs; As behaves distinctly due to its oxyanion form.
Sediment	PC1	51.65%	Cu, Zn, Cr (positive); Mn, Fe (negative)	Represents metal enrichment in sediments associated with anthropogenic inputs, contrasting with Mn–Fe oxide phases.
Sediment	PC2	37.51%	Al, Pb, As (negative); Cr, Ni (moderate positive)	Indicates lithogenic vs. anthropogenic source separation, suggesting grain-size control and adsorptive differences among metals.
Sediment	PC3	10.84%	Cu, Cr, Ni (minor positive loadings)	Accounts for minor variability linked to localized depositional or redox variations.

Figure 9 showcases a spatial distribution map created using ArcGIS-based Inverse Distance Weighting (IDW) to visualize contamination gradients along the Nwaniba River. The map identifies

hotspots near Sites 1 and A, suggesting upstream enrichment, while lower levels downstream indicate dilution and deposition. By overlaying matrices, the visualization emphasizes the connection between water and sediment, as well as metal-exchange zones, offering crucial insights into the river's environmental conditions (Luo *et al.,* 2025; Shyam *et al.,* 2022; Su *et al.,* 2023). The water–sediment overlay is shown in a comparative map in Figure 10, which additionally demonstrates locations with high metal concentrations that coincide and show the interaction between the particulate and dissolved phases. An important tool for environmental management and decision-making processes, this spatial correlation aids in identifying critical zones for planning repair and pollution control (Liu et al., 2016; Reimann et al., 2017; Shyam et al., 2022). The intricate, multi-faceted examination of trace-metal contamination in the Nwaniba River system sheds light on the various hydrological, geochemical, and human factors affecting metal distribution in water and sediment matrices (Azam *et al.,* 2023; Su *et al.,* 2023). Physicochemical parameters (Tables 1-2; Fig. 2) reveal that the Nwaniba River exhibits mild alkalinity to neutral pH (6.7-8.3 in water, 6.2-7.1 in sediments) and moderate electrical conductivity (36-85 µS/cm) with TDS values (< 50 mg/L). These measurements suggest low salinity but detectable ionic content, aligning with the characteristics of continental freshwater systems impacted by land-based inputs (Liu *et al.,* 2016). Elevated pH and conductivity levels near the estuarine outlet (Site 4) suggest saline intrusion and anthropogenic discharges.

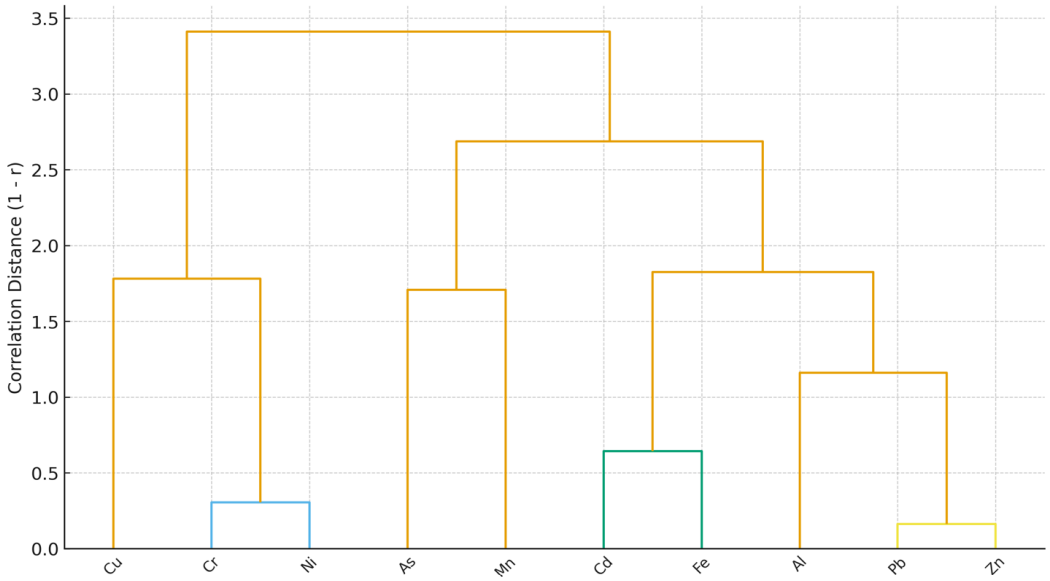

Figure 9: Dendrogram Showing Hierarchical Clustering of Trace Metals across Sampling Sites.

In sediments, an increase in organic matter content (3.8-5.1%) and clay enrichment downstream is observed, which improves the capacity for trace metal absorption (Ololade *et al.,* 2024). These baseline physicochemical patterns shape the geochemical environment where metals like Fe, Mn, Pb, Cu, Cr, and Ni exhibit varying behaviors across phases. Concentration data (Tables 3-4) highlight distinct differences between water and sediment compartments. In water, Fe (0.6291-3.1196 mg/L) and Mn (0.1023-0.1391 mg/L) predominate, with comparatively lower levels of Pb, Cr, and Cu, and non-detectable Cd. This indicates dilution during the wet season and partial precipitation of particle-

reactive metals. In contrast, sediments display substantial enrichment, with Mn levels reaching 2976.93 mg/kg and Pb exceeding 60 mg/kg at Site A. These values are consistent with polluted river systems affected by both natural rock-forming processes and human-induced inputs (Warczyk *et al.,* 2020). Elevated Fe and Mn concentrations indicate the prevalence of Fe–Mn oxides, which function as scavengers for trace metals, trapping contaminants that can be released again under specific conditions. This sediment enrichment suggests past accumulation and a potential source of secondary pollution during environmental shifts (Onojake *et al.,* 2017).

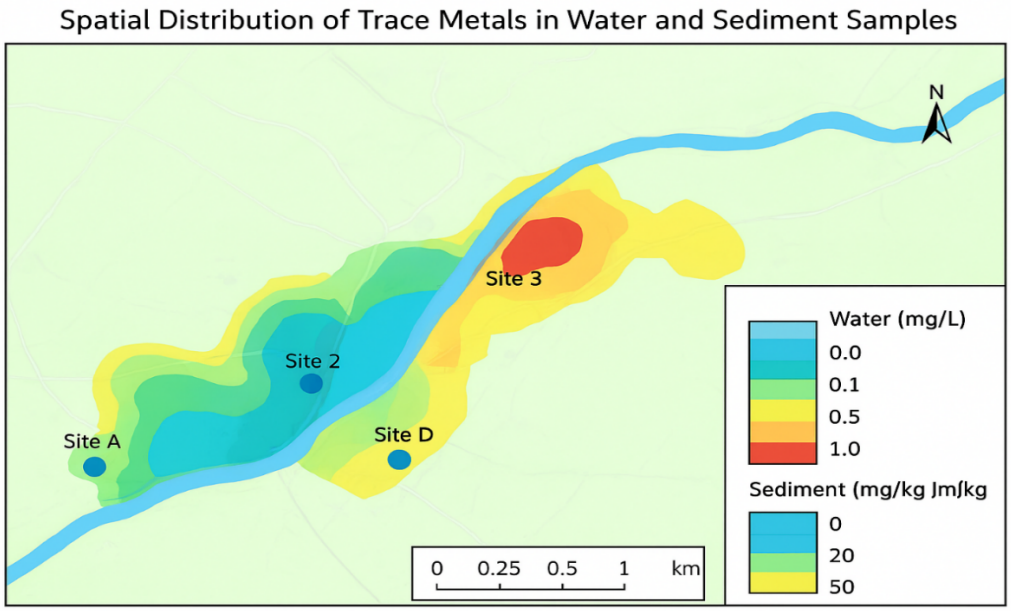

Figure 10: Spatial Distribution of Trace Metals in Water and Sediment Samples from Nwaniba River Using IDW Interpolation in ArcGIS 10.8

Machine learning analyses (Tables 5-6; Figs. 3-6) offered predictive insights into these distributions. For water, Random Forest (RF) produced a Root Mean Square Error (RMSE) of 0.7808, Support Vector Machine (SVM) yielded 0.5966, and Artificial Neural Network (ANN) resulted in 0.1163. This demonstrates the neural network's advanced capability to capture non-linear relationships among water-quality parameters and metal concentrations. The ANN's low error signifies its effectiveness in modeling Fe dynamics driven by intricate redox and pH interactions. On the other hand, sediment modeling showed higher RMSEs (RF = 257.42; SVM = 250.38; ANN = 303.78) due to the limited sample size and the diverse composition of sediments (Ghanbari *et al.,* 2020; Gholami *et al.,* 2019). Despite this, RF and SVM demonstrated robust performance, highlighting their dependability in predicting spatial variability across sites. These results echo global findings that hybrid machine learning approaches can enhance traditional geochemical evaluations by estimating uncertainty and prioritizing predictor significance (Kufel *et al.,* 2023b, 2023a; Nguyen *et al.,* 2019). The ANN loss curves (Figs. 4 and 6) offer additional confirmation of model convergence, underscoring the potential for machine learning-based early-warning systems for metal pollution detection and management. Descriptive statistics (Tables 7 and 10) accentuate the crucial role of Fe and Mn as key elements

influencing partitioning equilibria due to their redox-active nature, while Cu, Pb, and Cr exhibit significant variability, reflecting influences from both natural rock-forming processes and human activities. Low standard deviations for Cu and Zn in water point to steady dissolved fractions, whereas broad variations in sediment Mn and Cr suggest the influence of site-specific depositional energy and redox micro-environments (Akinpelu *et al.,* 2025). Correlation matrices (Tables 8 and 11; Figs. 7-8) demonstrate strong positive correlations between Fe, Mn, Cr, Ni, and Pb, indicating shared sources or common controlling factors like adsorption onto Fe/Mn oxides. These inter-element relationships confirm that Fe–Mn cycling primarily drives trace-metal mobility, with Cr–Ni correlations suggesting redox-linked substitution within oxide lattices. Conversely, weak correlations for As and Cd demonstrate distinct geochemical behaviors influenced by their oxyanion and soft-cation characteristics, respectively (Ololade *et al.,* 2024). Furthermore, Principal Component Analysis (PCA) results (Tables 9, 12, and 13) simplify the multidimensional data into significant orthogonal components that explain over 85% of the total variance. In water, PC1 (52.37%) separates a lithogenic–redox axis where Al, Cd, and Fe are contrasted with Cr and Ni, showcasing the interaction between natural mineral dissolution and redox-sensitive mobilization. PC2 (35.66%) isolates Pb and Zn as indicators of human influence, potentially from domestic or agricultural sources, while As behaves independently due to its oxyanion mobility under oxidizing conditions. For sediments, PC1 (51.65%) contrasts Cu–Zn–Cr enrichment with Fe–Mn oxide phases, illustrating the differences between human-induced accumulation and natural sorbent control. PC2 (37.51%) separates lithogenic elements (Al–Pb–As) from moderate Cr–Ni contributions, demonstrating the combined effects of grain size and depositional geochemistry. PC3 (10.84%) captures local anomalies in the deposition process. The PCA interpretation confirms that contamination is shaped by a combination of human and natural sources, aligning with the findings of Esenowo *et al.,* (2018) and (Ubong *et al.,* 2020). The dendrogram (Figure 9) supports PCA results, demonstrating two primary clusters: (i) Fe–Al–Cd–Pb–Zn, indicative of mixed geochemical or anthropogenic sources, and (ii) Cr–Ni–Mn, linked to lithogenic or redox-sensitive processes. This hierarchical structure suggests that metals with similar environmental behaviors are likely to accumulate together, an observation also noted in other Niger Delta River systems (Nor *et al.,* 2022). The geospatial visualization (Figure 10) adds further context, depicting spatial gradients where Sites A and 1 display high metal concentrations that decrease downstream towards the estuary. Anthropogenic inputs compound natural enrichment, as seen by the hotspot zones in the middle and southern reaches that correlate to human towns and agricultural activity. In contrast to sediment-bound pollutants, aqueous metals are still widely distributed, as indicated by the IDW interpolation surfaces, supporting the dual-compartment technique for thorough pollution evaluation. These comprehensive analyses also show that sediment texture, anthropogenic pressure, and physicochemical context all interact strongly. While organic matter and the amount of Fe–Mn oxide in sediments operate as both sinks and secondary sources, pH and redox potential play a major role in controlling water metals. Coherence between cluster-derived categories, PCA-defined latent structures, and RF-identified important predictors shows that multivariate statistics and machine learning agree on consistent geochemical interpretations. For river-system management, this supports the growing idea that data-driven analytics can supplement

conventional hydrogeochemistry (Koutsoukas *et al.,* 2017; Luo *et al.,* 2025; Nguyen *et al.,* 2019). Remediation efforts should concentrate on preserving oxic conditions to avoid remobilization in redox-buffering zones, which are identified by Fe–Mn-dominated clusters from a management standpoint. Waste discharges and surface runoff must be managed for Pb–Zn enhanced segments. Neural architectures may be able to predict seasonal or future contamination scenarios, which would help with proactive risk mitigation, according to the ANN model's improved performance (lowest RMSE = 0.1163). Since water represents real-time movement and sediments archive long-term contamination, the intimate link between water and sediment metal patterns emphasizes the necessity of integrated monitoring. In accordance with international best practices for riverine pollution assessment, the combined geospatial and statistical outputs offer a basis for creating focused intervention zones (Kufel *et al.,* 2023b; Warczyk *et al.,* 2020; Yalcin *et al.,* 2016). Additionally, the findings show that both increased human activity and natural lithogenic inputs contribute to the contamination of the Nwaniba River. Mechanistic pathways of adsorption, coprecipitation, and redox cycling are highlighted by metal associations like Cu–Zn–Cr and Fe–Mn–Ni. These relationships were quantitatively validated by machine-learning algorithms, and the underlying source patterns were clarified by PCA and clustering. The identification of contaminated hotspots by geospatial visualization highlighted the necessity of sediment treatment and catchment-wide pollution management. Taken together, these results confirm that a multi-statistical, machine-learning-based framework is an effective decision-support tool for sustainable river management and environmental surveying.

Conclusion

This research demonstrates that combining machine learning algorithms with geostatistical and multivariate approaches significantly enhances understanding of trace metal dynamics in aquatic systems. In the Nwaniba River, Random Forest, SVM, and ANN models effectively characterized relationships among physicochemical parameters and metal concentrations, identifying Fe, Mn, and Cr as dominant predictors of contamination. The superior performance of the ANN model indicates that neural networks can successfully model nonlinear environmental interactions that traditional methods often overlook. Statistical evaluations revealed strong Fe–Mn–Cr–Ni correlations, suggesting common redox-controlled pathways, while PCA and clustering distinguished lithogenic versus anthropogenic sources. Sediment analyses confirmed that metals such as Cu, Pb, and Cr accumulate due to agricultural and domestic discharges, whereas Fe and Mn oxides act as major sorbents controlling partitioning. Geospatial interpolation highlighted contamination hotspots upstream and gradual attenuation downstream, illustrating the dual roles of hydrodynamics and sediment texture in metal mobility. These findings emphasize that maintaining oxic conditions and regulating effluent discharge are vital for preventing metal remobilization and secondary pollution. Integrating geospatial, chemical, and machine-learning tools provides a robust framework for predicting contamination trends, identifying critical risk zones, and supporting policy formulation. The approach adopted here can be extended to other riverine systems to forecast future contamination scenarios and guide proactive remediation. Overall, this study contributes a scientifically rigorous

and data-driven methodology for assessing environmental health, advancing the use of artificial intelligence as a predictive and interpretive tool in sustainable river management.

References

Akinpelu, O. P., Gantayat, R. R., Elumalai, V., Li, P. (2025) Human and Ecological Risk Assessment: An International Probabilistic analysis of water quality deterioration and health risks assessment incorporating machine learning techniques in Mhlathuze catchment , South Africa. *Human and Ecological Risk Assessment: An International Journal*, *31*(5–6), 735–760. https://doi.org/10.1080/10807039.2025.2500382

Alam, G. M. I., Arfin Tanim, S., Sarker, S. K., Watanobe, Y., Islam, R., Mridha, M. F., Nur, K. (2025) Deep learning model based prediction of vehicle CO2 emissions with eXplainable AI integration for sustainable environment. *Scientific Reports*, *15*(1), 3655. https://doi.org/10.1038/s41598-025-87233-y

Azam, M. G., Hossain, M. A., Sarker, U., Alam, A. K. M. M., Nair, R. M., Roychowdhury, R., Ercisli, S., Golokhvast, K. S. (2023) Genetic Analyses of Mungbean [Vigna radiata (L.) Wilczek] Breeding Traits for Selecting Superior Genotype(s) Using Multivariate and Multi-Traits Indexing Approaches. *Plants*, *12*(10), 1984. https://doi.org/10.3390/plants12101984

Belbachir C., Aouniti A., Khamri M., Chafi A., Hammouti B. (2013) Heavy metals (copper, zinc, iron and cadmium) in sediments and the small clam (Chamelea gallina) of the coastal area north-east of Morocco, *J. Chem. Pharm. Res.,* 5(12), 1307-1314

Ding, Y., Wang, M., Fu, Y., Zhang, L., Wang, X. (2023) A Wildfire Detection Algorithm Based on the Dynamic Brightness Temperature Threshold. *Forests*, *14*(3), 477. https://doi.org/10.3390/f14030477

El Hammari L., Latifi S., Saoiabi S., Saoiabi A., Azzaoui K., *et al*. (2022), Toxic heavy metals removal from river water using a porous phospho-calcic hydroxyapatite, *Mor. J. Chem.* 10(1), 62-72, https://doi.org/10.48317/IMIST.PRSM/morjchem-v10i1.31752

Errich A., Salim R., El Hajjaji S., Azzaoui K., Hammouti B., Sabbahi R., Mandi L., Fekhaoui M. (2024) Multivariate analysis and A GIS-based method to assess surface water quality in the Sakia El Hamra River Near Laâyoune City, Morocco, *Mor. J. Chem.,* 12(3), 1192-1209, https://doi.org/10.48317/IMIST.PRSM/morjchem-v12i3.48643

Esenowo, I., Ugwumba, A., Akpan, A. (2018) Evaluating the Physico-chemical Characteristics and Plankton Diversity of Nwaniba River, South-South Nigeria. *Asian Journal of Environment & Ecology*, *5*(3), 1–8. https://doi.org/10.9734/ajee/2017/39038

Gerke, T. L., Little, B. J., Barry Maynard, J. (2016) Manganese deposition in drinking water distribution systems. *Science of The Total Environment*, *541*, 184–193. https://doi.org/10.1016/j.scitotenv.2015.09.054

Ghanbari, H., Jacques, O., Adaïmé, M.-É., Gregory-Eaves, I., Antoniades, D. (2020) Remote Sensing of Lake Sediment Core Particle Size Using Hyperspectral Image Analysis. *Remote Sensing*, *12*(23), 3850. https://doi.org/10.3390/rs12233850

Gholami, H., Jafari TakhtiNajad, E., Collins, A. L., Fathabadi, A. (2019) Monte Carlo fingerprinting of the terrestrial sources of different particle size fractions of coastal sediment deposits using

geochemical tracers: Some lessons for the user community. *Environmental Science and Pollution Research*, *26*(13), 13560–13579. https://doi.org/10.1007/s11356-019-04857-0

Hammoumi, D., Al-Aizari, H. S., Alaraidh, I. A., Okla, M. K., Assal, M. E., Al-Aizari, A. R., Moshab, M. S., Chakiri, S., Bejjaji, Z. (2024) Seasonal Variations and Assessment of Surface Water Quality Using Water Quality Index (WQI) and Principal Component Analysis (PCA): A Case Study. *Sustainability*, *16*(13), 5644. https://doi.org/10.3390/su16135644

Hammouti D., Elkari B., Thibault N., GadmerA., Rapadamnaba R., Ourabah L. (2025) Data visualization Project -report, *Afr. J. Manag. Engg. Technol.,* 3(2), 139-149

Hsu, L.-C., Huang, C.-Y., Chuang, Y.-H., Chen, H.-W., Chan, Y.-T., Teah, H. Y., Chen, T.-Y., Chang, C.-F., Liu, Y.-T., Tzou, Y.-M. (2016) Accumulation of heavy metals and trace elements in fluvial sediments received effluents from traditional and semiconductor industries. *Scientific Reports*, *6*(1), 34250. https://doi.org/10.1038/srep34250

Kabzińska, K., Szczesio, M., Świętosławski, J., Turek, A. (2015a) The effect of bottom sediments on the content of heavy metals in meadow soils. *Geology, Geophysics & Environment*, *41*(1), 25. https://doi.org/10.7494/geol.2015.41.1.25

Kabzińska, K., Szczesio, M., Świętosławski, J., Turek, A. (2015b) The effect of bottom sediments on the content of heavy metals in meadow soils. *Geology, Geophysics & Environment*, *41*(1), 25. https://doi.org/10.7494/geol.2015.41.1.25

Koutsoukas, A., Monaghan, K. J., Li, X., Huan, J. (2017) Deep-learning: Investigating deep neural networks hyper-parameters and comparison of performance to shallow methods for modeling bioactivity data. *Journal of Cheminformatics*, *9*(1), 1–13. https://doi.org/10.1186/s13321-017-0226-y

Kufel, J., Bargieł-Łączek, K., Kocot, S., Koźlik, M., Bartnikowska, W., Janik, M., Czogalik, Ł., Dudek, P., Magiera, M., Lis, A., Paszkiewicz, I., Nawrat, Z., Cebula, M., Gruszczyńska, K. (2023a) What Is Machine Learning, Artificial Neural Networks and Deep Learning?—Examples of Practical Applications in Medicine. *Diagnostics*, *13*(15). https://doi.org/10.3390/diagnostics13152582

Kufel, J., Bargieł-Łączek, K., Kocot, S., Koźlik, M., Bartnikowska, W., Janik, M., Czogalik, Ł., Dudek, P., Magiera, M., Lis, A., Paszkiewicz, I., Nawrat, Z., Cebula, M., Gruszczyńska, K. (2023b) What Is Machine Learning, Artificial Neural Networks and Deep Learning?—Examples of Practical Applications in Medicine. *Diagnostics*, *13*(15), 2582. https://doi.org/10.3390/diagnostics13152582

Liu, Y., Cheng, Q., Zhou, K., Xia, Q., Wang, X. (2016) Multivariate analysis for geochemical process identification using stream sediment geochemical data: A perspective from compositional data. *Geochemical Journal*, *50*(4), 293–314. https://doi.org/10.2343/geochemj.2.0415

Luo, Y., Peng, B., Li, T., Chang, M., Guo, Y., Liu, Y., Nie, X. (2025) Agricultural Activities and Hydrological Processes Drive Nitrogen Pollution and Transport in Polder Waters: Evidence from Hydrochemical and Isotopic Analysis. *Water*, *17*(17), 2601. https://doi.org/10.3390/w17172601

Marsidi, N., Abu Hasan, H., Sheikh Abdullah, S. R. (2018) A review of biological aerated filters for iron and manganese ions removal in water treatment. *Journal of Water Process Engineering*, *23*, 1–12. https://doi.org/10.1016/j.jwpe.2018.01.010

Nguyen, G., Dlugolinsky, S., Bobák, M., Tran, V., López García, Á., Heredia, I., Malík, P., Hluchý, L. (2019) Machine Learning and Deep Learning frameworks and libraries for large-scale data mining: A survey. *Artificial Intelligence Review*, *52*(1), 77–124. https://doi.org/10.1007/s10462-018-09679-z

Nor, S. M. M., Jaafar, M., Jaafar, N. M. S. N., Redzuan, N. S., Omar, W. B. W., Deraman, M. Y., Azli, S. N. S. N., Shehrom, N. A., Mahyudin, 'Ainna, Bahari, N. A., Zulkafli, N. N., Jaafar, N. F., Ma'ad, S. N. S., Zamri, M. I. M., Amirudin, A., Abdullah, N. A., Zakaria, N. (2022) Dataset of physico-chemical water parameters, phytoplankton, flora and fauna in mangrove ecosystem at Sungai Kertih, Terengganu, Malaysia. *Data in Brief*, *42*, 108096. https://doi.org/10.1016/j.dib.2022.108096

Obadimu, C. O., Shaibu, S. E., Ekwere, I. O., Adelagun, R. O. A. (2024) Machine Learning-Based Forecasting Of Bioaccumulation and Histopathological Effects In Aquatic Organisms. *Fudma Journal of Sciences*, *8*(6), 485–496. https://doi.org/10.33003/fjs-2024-0806-3002

Obadimu, C. O., Shaibu, S. E., Enin, G. N., Ituen, E. B., Anweting, I. B., Ubong, U. U., Ekwere, I. O., Adewusi, S. G., Adeoye, T. J., Fapojuwo, D. P., Ofon, U. A., Fatunla, O. K., Essien, N. S., Audu, Oluwatosin. Y., Tshentu, Z. R., Nelana, S. M., Klink, M. J., Ayanda, O. S. (2024) Aqueous phase adsorption of phenothiazine derivative onto zinc oxide doped activated carbon. *Scientific Reports*, *14*(1), 21611. https://doi.org/10.1038/s41598-024-71196-7

Olden J.D., Joshua J. Lawler J.J. and Poff N.L. (2008) Machine Learning Methods Without Tears: A Primer for Ecologists, *The Quarterly Review of Biology*, 83, No. 2, 171-193 Published by: The University of Chicago Press Stable URL: https://www.jstor.org/stable/10.1086/587826

Ololade, I. A., Apata, A., Oladoja, N. A., Alabi, B. A., Ololade, O. O. (2024) Appraisal of river sediments in southwestern Nigeria with a special focus on trace metals: Occurrence, seasonal variation, sources, and health risks. *Ecological Frontiers*, *44*(1), 155–166.

Onojake, M. C., Sikoki, F. D., Omokheyeke, O., Akpiri, R. U. (2017) Surface water characteristics and trace metals level of the Bonny/New Calabar River Estuary, Niger Delta, Nigeria. *Applied Water Science*, *7*(2), 951–959. https://doi.org/10.1007/s13201-015-0306-y

Oyem, H. H., Oyem, I. M., Usese, A. I. (2015) Iron, manganese, cadmium, chromium, zinc and arsenic groundwater contents of Agbor and Owa communities of Nigeria. *SpringerPlus*, *4*(1), 104. https://doi.org/10.1186/s40064-015-0867-0

Peng, W., Li, X., Xiao, S., Fan, W. (2018) Review of remediation technologies for sediments contaminated by heavy metals. *Journal of Soils and Sediments*, *18*(4), 1701–1719. https://doi.org/10.1007/s11368-018-1921-7

Reimann, C., Filzmoser, P., Hron, K., Kynčlová, P., Garrett, R. G. (2017) A new method for correlation analysis of compositional (environmental) data – a worked example. *Science of The Total Environment*, *607–608*, 965–971. https://doi.org/10.1016/j.scitotenv.2017.06.063

Rodrigues, P. C., Awe, O. O., Pimentel, J. S., Mahmoudvand, R. (2020) Modelling the Behaviour of Currency Exchange Rates with Singular Spectrum Analysis and Artificial Neural Networks. *Stats*, *3*(2), 137–157. https://doi.org/10.3390/stats3020012

Salari, M., Salami Shahid, E., Afzali, S. H., Ehteshami, M., Conti, G. O., Derakhshan, Z., Sheibani, S. N. (2018) Quality assessment and artificial neural networks modeling for characterization of chemical and physical parameters of potable water. *Food and Chemical Toxicology*, *118*, 212–219. https://doi.org/10.1016/j.fct.2018.04.036

Sarker, I.H. (2021). Machine Learning: Algorithms, Real-World Applications and Research Directions. SN *Comput. Sci.* 2, 160, https://doi.org/10.1007/s42979-021-00592-x

Sharifuzzaman S.M., Rahman H., Ashekuzzaman S.M., Islam M.M., Chowdhury S.R., Hossain M.S. (2016) Heavy Metals Accumulation in Coastal Sediments. In H. Hasegawa, I. Md. M. Rahman & M.A. Rahman (Eds.), *Environmental Remediation Technologies for Metal-Contaminated Soils* (pp. 21–42). Springer Japan. https://doi.org/10.1007/978-4-431-55759-3_2

Shyam, M., Meraj, G., Kanga, S., Sudhanshu, Farooq, M., Singh, S. K., Sahu, N., Kumar, P. (2022) Assessing the Groundwater Reserves of the Udaipur District, Aravalli Range, India, Using Geospatial Techniques. *Water*, *14*(4), 648. https://doi.org/10.3390/w14040648

Su, Q., Yu, H., Xu, X., Chen, B., Yang, L., Fu, T., Liu, W., Chen, G. (2023) Using Principal Component Analysis (PCA) Combined with Multivariate Change-Point Analysis to Identify Brine Layers Based on the Geochemistry of the Core Sediment. *Water*, *15*(10), 1926. https://doi.org/10.3390/w15101926

Ubong, U. U., Ekwere, I. O., Ikpe, E. E. (2020) Risk and Toxicity Assessments of Heavy Metals in Tympanotonus fuscatus and Sediments from Iko River, Akwa Ibom State, Nigeria. *International Journal of Environment and Climate Change*, *April*, 38–47. https://doi.org/10.9734/ijecc/2020/v10i330186

Ukut, M. O., Ibuotenang, N. D., Sunny, H. K., Uwah, E. I., Udotong, U. F., Ukpong, E. G., Shaibu, S. E. (2025) *Hydrological Harmony: Unlocking the Potential of Water Reuse and Recycling in Urban Ecosystems*. 1–12.

Warczyk, A., Wanic, T., Antonkiewicz, J., Pietrzykowski, M. (2020) Concentration of trace elements in forest soil affected by former timber depot. *Environmental Monitoring and Assessment*, *192*(10). https://doi.org/10.1007/s10661-020-08479-9

Witten, I. H., Frank, Eibe., Hall, M. A., Pal, C. J. (2017) CHAPTER 10. Deep learning. In *Data mining—Practical machine learning tools and techniques*.

Wojtkowska, M., Bogacki, J., Witeska, A. (2016) Assessment of the hazard posed by metal forms in water and sediments. *Science of The Total Environment*, *551–552*, 387–392. https://doi.org/10.1016/j.scitotenv.2016.01.073

Xu, Q., Wu, B., Chai, X. (2022) In Situ Remediation Technology for Heavy Metal Contaminated Sediment: A Review. *International Journal of Environmental Research and Public Health*, *19*(24), 16767. https://doi.org/10.3390/ijerph192416767

Yalcin, F., Kilic, S., Nyamsari, D., Yalcin, M., Kilic, M. (2016) Principal Component Analysis of Integrated Metal Concentrations of Bogacayi Riverbank Sediments in Turkey. *Polish Journal of Environmental Studies*, *25*(2), 471–485. https://doi.org/10.15244/pjoes/61009

Zajusz-Zubek, E., Mainka, A., Kaczmarek, K. (2023) Dendrograms, heat maps and principal component analysis – the practical use of statistical methods for source apportionment of trace elements in PM10. *Journal of Environmental Science and Health, Part A*, *58*(3), 163–170. https://doi.org/10.1080/10934529.2019.1670026

Zhou, T., Wang, F., Yang, Z. (2017) Comparative Analysis of ANN and SVM Models Combined with Wavelet Preprocess for Groundwater Depth Prediction. *Water*, *9*(10), 781. https://doi.org/10.3390/w9100781

(2025) ; http://www.jmaterenvironsci.com